A role of the endoplasmic reticulum in a mathematical model of corticotroph action potentials

Paul R. Shorten[*], **Andrew P. LeBeau**[†] **A. Bruce Robson**[‡], **Alan E. McKinnon**[‡], **and David J.N. Wall**[*]

[*] *Biomathematics Research Centre, Department of Mathematics & Statistics, University of Canterbury, Private Bag 4800, Christchurch, New Zealand.*

Report Number: 173 November 1998

Keywords: CRH, Ion channels, Calcium, Potassium, Hodgkin-Huxley, ACTH

[†] *Mathematical Research Branch, NIDDK, National Institutes of Health, Bethesda, MD 20892, USA.*

[‡] *Applied Computing, Mathematics and Statistics Group, Division of Applied Management and Computing, PO Box 84, Lincoln University, Canterbury, New Zealand.*

Abstract

Pituitary corticotroph cells generate repetitive action potentials and associated Ca^{2+} transients in response to the agonist corticotropin releasing hormone (CRH). There is indirect evidence suggesting that the agonist, by way of complex intracellular mechanisms, modulates the voltage sensitivity of the L-type Ca^{2+} channels embedded in the plasma membrane. We have previously constructed a Hodgkin-Huxley type model of this process, which indicated that an increase in the L-type Ca^{2+} current is sufficient to generate repetitive action potentials [LeBeau et al. (1997). Biophysical Journal 73, 1263-1275].

In this paper we extend our model by including more realistic Ca^{2+} transport between cytosolic and endoplasmic compartments, and spatial variation in our description of the endoplasmic reticulum (ER) and cytosolic $[Ca^{2+}]$. We have found firstly that this $[Ca^{2+}]$ spatial variation did not significantly affect the generation of action potentials, and secondly that a gradual increase in the ER Ca^{2+} during repetitive action potential activity can ultimately feed back sufficient Ca^{2+} into the cytosol to eliminate action potentials. We discuss ways in which cells might regulate their intracellular $[Ca^{2+}]$ dynamics to avoid such an effect.

Introduction

CRH is one of the major regulatory hormones linked with the neuroendocrine response to stress (Rivier and Vale, 1983; Gibbs, 1985; Jones and Gillham, 1988). Secreted from CRH-neurons in the paraventricular nucleus of the hypothalamus, CRH travels through the hypothalmo-pituitary portal system to the anterior pituitary (Merchenthaler et al., 1984; Plotsky et al., 1985; Whitnall et al., 1985; Plotsky and Sawchenko, 1987), stimulating the secretion of adrenocorticotropic hormone (ACTH) and other biologically significant hormones from the corticotroph cell population (Antoni, 1986; Rivier and Plotsky, 1986; Jones and Gillham, 1988). Secreted ACTH then initiates the release of adrenal glucocorticoids, which help the body reduce the metabolic demands of stress. These glucocorticoids also provide a negative feedback mechanism, inhibiting the secretory process at the pituitary and hypothalamus (Bilezikjian and Vale, 1983; Keller-Wood and Dallman, 1984; Widmaier and Dallman, 1984).

The intracellular mechanisms underlying the control of ACTH secretion in response to CRH have been only partially characterised. However CRH is known to activate the adenosine 3',5'-cyclic monophosphate (cAMP) dependent protein kinase A (PKA) pathway (Labrie et al., 1982; Aguilera et al., 1983; Reisine et al., 1986; Kuryshev et al., 1995b). The phosphorylation targets for PKA in corticotrophs have not been identified, however PKA is known to phosphorylate L-type voltage dependent Ca^{2+} channels (Mundiña-Weilenmann et al., 1991; Hille, 1992; Sculptoreanu et al., 1993). CRH also induces a membrane depolarization (Mollard et al., 1987), which is associated with the generation of action potentials in quiescent corticotrophs, and the enhancement of action potential frequency in spontaneously active corticotrophs (Guérineau et al., 1991; Kuryshev et al., 1996). Associated with the action potentials are Ca^{2+} transients, predominately, if not totally, arising due to Ca^{2+} influx via L-type Ca^{2+} channels (Kuryshev et al., 1996). H-89, an inhibitor of PKA, significantly attenuates CRH-induced action potentials (Kuryshev et al., 1995b), demonstrating a major role for PKA in mediating the changes in electrical excitability and Ca^{2+}-mobilising actions of CRH. There is thus indirect evidence supporting the hypothesis of a CRH-induced PKA-dependent phosphorylation of the L-type Ca^{2+} channels (LeBeau et al., 1997), resulting in action potentials, and Ca^{2+} transients. The model introduced in LeBeau et al. (1997) is central to our discussion; we henceforth denote it by (I).

Ca^{2+} has been well established as an important intracellular trigger for hormone secretion (Tsien and Tsien, 1990; Clapham, 1995). The spatio-temporal patterns in cytosolic Ca^{2+}, generated by the subtle interplay between cellular Ca^{2+} sources and removal mechanisms, are believed to be an integral part of the exocytotic pathway (Meyer and Stryer, 1991). For this reason the study of Ca^{2+} transport and cell electrical activity provides insight into the stimulus secretion pathway. We have previously constructed a mathematical model of the major plasma membrane ionic currents and the associated intracellular Ca^{2+} dynamics identified in corticotrophs (I). For model simplicity, we originally assumed that the intracellular free Ca^{2+} concentration ($[Ca^{2+}]_i$) was spatially uniform, and instantly mixed. The ER Ca^{2+} storage capacity was assumed to be large, and the amount of Ca^{2+} stored in the ER was assumed to vary negligibly during action potentials. We found that an increase in the L-type current was sufficient to generate repetitive action potentials from a previously resting state of the model. The increase in the L-type current could be elicited by either a shift in the voltage dependence of the current to more negative potentials, or by an increase in the conductance. In the current paper we extend our previous model by including two new components. Firstly,

we allow bidirectional Ca^{2+} transport between the cytosol and a finite, dynamic ER store. Secondly, along with other workers (Atri et al., 1993; Li et al., 1997), because the Ca^{2+}-sensing components of the cell have both different sensitivities to Ca^{2+} and different spatial locations, we consider spatially varying Ca^{2+}. We investigate what effects these two changes have on the model dynamics.

The original model

The original model (I) is of Hodgkin-Huxley form (Hodgkin and Huxley, 1952), and consists of six coupled ordinary differential equations. The model description is similar to the models of Li et al. (1995, 1997), which investigated electrical activity in pituitary gonadotroph cells. For our corticotroph model the potential difference (V) across the plasma membrane satisfies

$$c_{\mathrm{m}}\frac{dV}{dt} = -(I_{\mathrm{Ca-L}} + I_{\mathrm{Ca-T}} + I_{\mathrm{K-DR}} + I_{\mathrm{K-Ca}} + I_{\mathrm{Leak}}), \tag{1}$$

where c_{m} is the cell surface membrane capacitance (see Table 1 for parameter values). Four ionic currents are included in the model: 1) a high voltage threshold dihydropyridine sensitive L-type Ca^{2+} current ($I_{\mathrm{Ca-L}}$), responsible for most of the inward Ca^{2+} current during an action potential; 2) a low voltage threshold rapidly inactivating T-type voltage sensitive Ca^{2+} current ($I_{\mathrm{Ca-T}}$); 3) a voltage-sensitive K^+ current ($I_{\mathrm{K-DR}}$), predominantly responsible for the action potential repolarization; and 4) a Ca^{2+}-activated K^+ current ($I_{\mathrm{K-Ca}}$). The remaining leak current (I_{Leak}) represents all other ionic current contributions not specifically described. We have previously described the construction of these model ionic currents from electrophysiological measurements in corticotrophs (I).

There is evidence suggesting the existence of other channel types in corticotrophs, including: 1) TTX-sensitive Na^+ channels (Kuryshev et al., 1996); 2) P-type Ca^{2+} channels, contributing to the regulation of firing frequency (Kuryshev et al., 1995a; Kuryshev et al., 1996); 3) an inward rectifier K^+ current (Kuryshev et al., 1997), contributing to the maintenance of the resting membrane potential; and 4) a nonselective cation current (Takano et al., 1996). However these channels are not well characterised in corticotrophs and our desire is to investigate the basic mechanisms of action potential generation and calcium signalling with as simple a model as possible. Thus we do not include a description of these other channels in the model presented here.

The ER model

The ER Ca^{2+} store performs a number of important cellular functions, including cellular Ca^{2+} homeostasis and protein synthesis (Alberts et al., 1983, p335). In this section we extend our original model (I) to include bidirectional Ca^{2+} transport between the cytosolic and ER compartments. This allows Ca^{2+} that has been sequestered by the ER to be released back into the cytosol, a feature that was not incorporated into (I).

The model

We model the cell as a spherical body, bounded by a plasma membrane containing Ca^{2+}-ATPase pumps and various ionic currents as outlined above. A schematic diagram of the

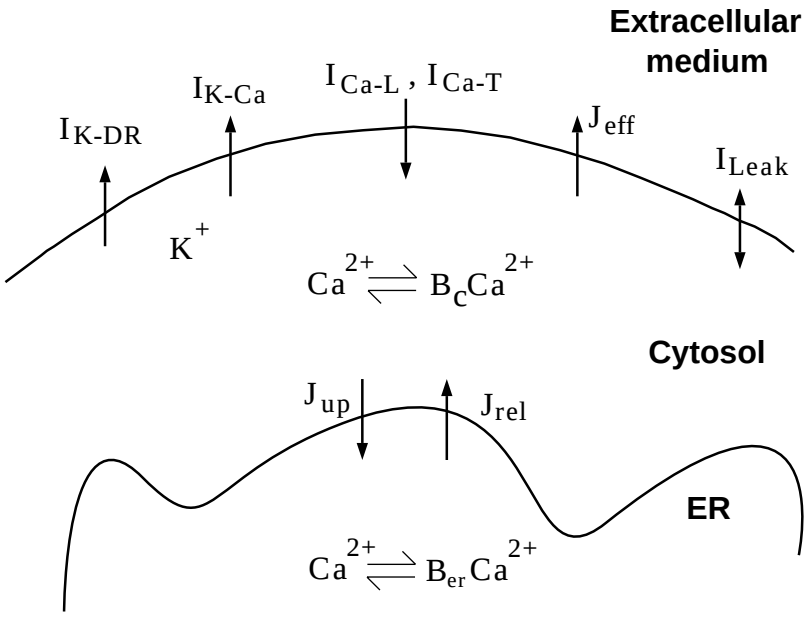

Figure 1: Schematic diagram of the ionic pathways included in the model. Three compartments are distinguished, the cytosol, the ER, and the extracellular medium. Bold arrows indicate the various channels and pumps. Within the ER and cytosolic compartments, significant portions of Ca^{2+} are bound to buffers, denoted by B_{er} and B_c respectively. Four ionic currents are included in the model: an L-type voltage sensitive Ca^{2+} current I_{Ca-L}, a fast inactivating T-type voltage sensitive Ca^{2+} current I_{Ca-T}, a voltage-sensitive K^+ current I_{K-DR}, and a non-voltage sensitive Ca^{2+}-activated K^+ current I_{K-Ca}. The remaining leak current I_{Leak} represents all other ionic current contributions. Also indicated are the plasma membrane and ER Ca^{2+}-ATPase pumps, J_{eff} and J_{up} respectively, along with an ER Ca^{2+} leakage term J_{rel}.

various ionic transport processes is shown in Fig. 1. It is assumed that the ER is distributed homogeneously throughout the cell, and shares the intracellular volume with the cytosol. The ER and cytosolic compartments are of different volumes V_{er} and V_c respectively, where the ER is assumed to fill 15% of the cell volume (Alberts et al., 1983, p320).

The compartments also have different buffering kinetics, (Li et al., 1997) given by f_{er} and f_{cyt}, the fraction of unbuffered Ca^{2+} in the respective volumes. This fraction is dependent on the concentration of buffer sites, their individual binding kinetics, and the $[Ca^{2+}]$ in the corresponding compartment (Wagner and Keizer, 1994). The precise nature of these Ca^{2+} buffers, each with unique binding kinetics is as yet undetermined, hence our model of Ca^{2+} buffering is simple. Assuming that the Ca^{2+} buffer concentration is suitably large relative to the $[Ca^{2+}]$ in the respective compartments (Jafri and Keizer, 1995), and the buffer kinetics are fast and in equilibrium at all times, it follows that the functional dependence of f_{er} and f_{cyt} on $[Ca^{2+}]$ will be weak, and can thus be treated as constant. In the cytosol, approximately 99% of Ca^{2+} is bound to buffers (Neher and Augustine, 1992; Tse et al., 1994), hence $f_{cyt} = 0.01$. The buffering of Ca^{2+} in the ER is assumed to be four times greater than in the cytosol (Li

et al., 1997), hence $f_{\mathrm{er}} = 0.0025$. (See Table 1)

There is no evidence to suggest that CRH, by means of a secondary messenger, directly induces the release of Ca^{2+} from the ER. Therefore, assuming the diffusive surface flux across the ER membrane is described by Fick's law, the leak current from the ER can be described by

$$J_{\mathrm{rel}} = P([Ca^{2+}]_{\mathrm{er}} - [Ca^{2+}]_{\mathrm{i}}), \tag{2}$$

where P is the ER membrane leak permeability, $[Ca^{2+}]_{\mathrm{er}}$ is the concentration of free Ca^{2+} in the ER, and $[Ca^{2+}]_{\mathrm{i}}$ is the concentration of free Ca^{2+} in the cytosol. Ca^{2+}-ATPase pumps are located on the surface of the ER membrane, allowing the cell to remove cytosolic Ca^{2+}. The uptake of Ca^{2+} into the ER is described by Michaelis-Menten kinetics (Lytton et al., 1992)

$$J_{\mathrm{up}} = \frac{\nu_{\mathrm{er}}[Ca^{2+}]_{\mathrm{i}}{}^2}{[Ca^{2+}]_{\mathrm{i}}{}^2 + K_{\mathrm{er}}^2}, \tag{3}$$

where ν_{er} is the maximum pump rate and K_{er} is the $[Ca^{2+}]_{\mathrm{i}}$ for half maximal pump activity.

Ca^{2+} influx through voltage sensitive Ca^{2+} channels (J_{in}), and efflux via the plasma membrane Ca^{2+}-ATPase pump (J_{eff}) are given by

$$J_{\mathrm{in}} = -\alpha(I_{\mathrm{Ca-L}} + I_{\mathrm{Ca-T}}), \tag{4}$$

$$J_{\mathrm{eff}} = \frac{\nu_{\mathrm{p}}[Ca^{2+}]_{\mathrm{i}}{}^2}{[Ca^{2+}]_{\mathrm{i}}{}^2 + K_{\mathrm{p}}^2}, \tag{5}$$

respectively, where α converts a Ca^{2+} ionic current into a Ca^{2+} flux density, ν_{p} is the maximum pump rate, and K_{p} is the $[Ca^{2+}]_{\mathrm{i}}$ for which the pump is half-maximally activated (see Table 1).

Parameter	Definition	Value	Source
c_{m}	Cell membrane capacitance	7 pF	(I)
$\mathrm{d}_{\mathrm{cell}}$	Cell diameter	15 μm	(I)
V_{cell}	Cell volume	1.77 pL	$1/6\pi \mathrm{d}_{\mathrm{cell}}{}^3$
V_{c}	Cytosolic volume	0.85 V_{cell}	(Alberts et al., 1983)
V_{er}	ER volume	0.15 V_{cell}	(Alberts et al., 1983)
A_{cell}	Cell surface area	707 $\mu\mathrm{m}^2$	$\pi \mathrm{d}_{\mathrm{cell}}{}^2$
f_{cyt}	Cytosolic Ca^{2+} buffering factor	0.01	(Neher and Augustine, 1992)
f_{er}	ER Ca^{2+} buffering factor	0.0025	(Li et al., 1997)
α	Ca^{2+} current to flux density conversion factor	0.0074 $\mu\mathrm{M}\cdot\mu\mathrm{m}\cdot\mathrm{ms}^{-1}\cdot\mathrm{pA}^{-1}$	$1/(z_{\mathrm{Ca}}FA_{\mathrm{cell}})$
β	Ratio of cell surface area to cytosolic volume	0.47 μm^{-1}	$A_{\mathrm{cell}}/V_{\mathrm{c}}$
P	ER permeability	0.0012 $\mathrm{pL}\cdot\mathrm{ms}^{-1}$	This paper
ν_{er}	Maximum ER Ca^{2+}-ATPase current	0.05 $\mu\mathrm{M}\cdot\mathrm{pL}\cdot\mathrm{ms}^{-1}$	This paper
K_{er}	$[Ca^{2+}]_{\mathrm{i}}$ for half maximal pump activity	0.2 μM	(Li et al., 1997)
ν_{p}	Maximum plasma membrane Ca^{2+}-ATPase flux	0.05 $\mu\mathrm{M}\cdot\mu\mathrm{m}\cdot\mathrm{ms}^{-1}$	(I)
K_{p}	$[Ca^{2+}]_{\mathrm{i}}$ for half maximal pump activity	0.08 μM	(I)
$V_{\mathrm{m_L}}$	L-type Ca^{2+} channel midpoint factor	-12 mV	(I)
D_{c}	Cytosolic Ca^{2+} diffusion coefficient	20 $\mu\mathrm{m}^2\cdot\mathrm{s}^{-1}$	(Wagner and Keizer, 1994)
D_{er}	ER Ca^{2+} diffusion coefficient	5 $\mu\mathrm{m}^2\cdot\mathrm{s}^{-1}$	(Li et al., 1997)

Table 1: Table of relevant model parameters.

Because of Ca^{2+} buffering the current ($J_{\mathrm{rel}} - J_{\mathrm{up}}$), representing the Ca^{2+} exchange across the ER membrane, must be multiplied by $f_{\mathrm{cyt}}/V_{\mathrm{c}}$ to produce the rate of concentration accu-

mulation in the cytosol *. The differential equation for $[Ca^{2+}]_i$ is then given by

$$\frac{d[Ca^{2+}]_i}{dt} = \frac{f_{cyt}}{V_c}(J_{rel} - J_{up}) + f_{cyt}\beta(J_{in} - J_{eff}), \tag{6}$$

where β is the ratio of cell surface area to cytosolic volume, relating ionic fluxes in the plasma membrane to the rate of intracellular concentration accumulation. The differential equation for the ER dynamics is similar to Eq. 6, but the ER is assumed not to interact directly with the extracellular medium, and the rate of concentration accumulation in the ER is now moderated by the factor f_{er}/V_{er} so yielding

$$\frac{d[Ca^{2+}]_{er}}{dt} = -\frac{f_{er}}{V_{er}}(J_{rel} - J_{up}). \tag{7}$$

The value for $[Ca^{2+}]_{er}$ at rest has not been determined, but we can estimate a lower bound from previously published experimental data. The agonist arginine vasopressin is thought to induce intracellular inositol trisphosphate (IP_3) production which binds to receptors located on the ER membrane and causes release of stored Ca^{2+} from the ER (Won and Orth, 1995). Single cell measurements of Ca^{2+} have shown that arginine vasopressin can generate a transient $[Ca^{2+}]_i$ response of up to 3μM (Corcuff et al., 1993). By use of the values for the relative volumes and buffering capacities we use (see Table 1) this gives a lower estimate for the resting $[Ca^{2+}]_{er}$ of 6-10 μM. At equilibrium we require that there be no net Ca^{2+} exchange between the cytosol and the ER. This allows us to find, using Eqs. 2 and 3, a linear functional relationship between ν_{er} and P. Our chosen leak permeability of $P = 0.0012$ pL $\cdot$ ms^{-1} then indicates that $\nu_{er} = 0.05$ μM $\cdot$ pL $\cdot$ ms^{-1}.

Numerical Methods

The system of ordinary differential equations (Eq. 1, Eq. 6 and Eq. 7, along with the equations associated with the channel activation gating variables (I)) were solved using a stiff system solver in the numerical package XPPAUT(3.0) †. Bifurcation diagrams were computed using AUTO (Doedel, 1981), as incorporated in XPPAUT.

Model behaviour

Experimentally, application of cAMP has been shown to increase the whole-cell Ca^{2+} current in corticotroph tumour cells (Luini et al., 1985). We have shown (I) that such an increase in the current can be generated either by an increase in the macroscopic conductance or by a shift in the voltage-sensitivity of the L-type Ca^{2+} current to more hyperpolarised potentials, the latter effect having experimental support from other cell-types (Nargeot et al., 1983; Mundiña-Weilenmann et al., 1991; Sculptoreanu et al., 1993). In the model, both effects led to the generation of repetitively firing action potentials. At present, it would seem that neither the currently available experimental data, nor the model, can resolve which, if any, of these mechanisms genuinely underlies action potential generation in response to CRH. Previously we arbitrarily chose to use a shift in the voltage-dependence of the L-type Ca^{2+} current but

*It should be noted that $(J_{rel} - J_{up})$ is an ionic current whereas $(J_{in} - J_{eff})$ is an ionic surface flux, thus ν_{er} and ν_p have different units.

†Written by Bard Ermentrout, and available at ftp.math.pitt.edu/pub/bardware

noted that an increase in the macroscopic conductance always produced very similar results (I). We continue with the same choice in the following analysis. The model parameter that controls the voltage-sensitivity of the L-type current is V_{m_L} (as described in (I)). Analysis of experimental data suggested a control V_{m_L} value of -12 mV under rest conditions, and we typically used a negative shift of 6 – 8 mV to generate action potentials (I).

With the addition of more realistic Ca^{2+} handling in the ER-model, described above, we wish to compare its behaviour with the original model (I). The ER-model resting state is similar to that in the original model; at equilibrium the $[Ca^{2+}]_i$ is 0.12 μM, $[Ca^{2+}]_{er}$ is 10.8 μM and the plasma membrane potential difference V is -56.1 mV. At equilibrium in the original model the $[Ca^{2+}]_i$ is 0.1 μM, with a plasma membrane potential difference of -54.8 mV. Fig. 2 compares ER-model simulations (—) with those from the original model (– – –), in which the voltage dependence of the L-type Ca^{2+} current activation is shifted to more negative potentials by changing V_{m_L} from -12 mV to -18 mV. This generates action potentials, and associated $[Ca^{2+}]_i$ transients in both models. The period of oscillations in both models is dependent on the rate of clearance of Ca^{2+} from the cytosol (i.e., due to the gradual removal of the hyperpolarizing influence of the Ca^{2+}-activated K^+ current). Our choice of parameters governing bidirectional flow of Ca^{2+} between the cytosol and ER resulted in an approximately 50% increase in the period of oscillations compared with the original model. However, the characteristics of the action potentials and $[Ca^{2+}]_i$ transients in the ER model are similar to those in the original model. The slower period is actually more consistent with experimentally observed activity (Guérineau et al., 1991; Kuryshev et al., 1996). The model $[Ca^{2+}]_i$ profiles display kinetic features similar to the experimental data (Guérineau et al., 1991), such as a rapid rising phase, and a slower falling phase where $[Ca^{2+}]_i$ falls most of the way back to its basal value before the next action potential. The action potentials display typical experimentally observed features, such as a rapid upstroke, a rapid downstroke which overshoots the resting potential, and a slow ramping hyperpolarization, leading to the firing of the next action potential.

During the train of action potentials in the ER model, $[Ca^{2+}]_{er}$ slowly increases (Fig. 2 C), as the ER sequesters Ca^{2+} and therefore acts to buffer the $[Ca^{2+}]_i$. If only a single transient were generated, the additional ER Ca^{2+} would be returned to the cytosol, and eventually removed from the cell altogether, to recover cellular $[Ca^{2+}]$ homeostasis. However, (Fig. 2 C) shows that with repetitive action potential activity, $[Ca^{2+}]_{er}$ builds up as each transient contributes additional Ca^{2+} to the cytosol.

The ER model behaves in a similar fashion to the original model for short periods of time. However an interesting behaviour is exhibited when we view the ER model over a longer period of time. Fig. 3 shows a model simulation over 70 s, where a negative shift in the voltage dependence of the L-type Ca^{2+} current from -12 mV to -18 mV generates action potentials, and associated $[Ca^{2+}]_i$ transients. During $[Ca^{2+}]_i$ oscillations, $[Ca^{2+}]_{er}$ rises slowly to approximately 15.8 μM after 70 s (Fig. 3 C). Coupled to the buildup in $[Ca^{2+}]_{er}$ is a gradual rise in the average $[Ca^{2+}]_i$ (i.e., averaged over the course of a transient) and a slight decrease in the amplitude and frequency of $[Ca^{2+}]_i$ oscillations. The slow but steady rise in $[Ca^{2+}]_i$ results from an enhanced leak from the ER and leads to a gradual increase in the average activation of I_{K-Ca}. This in turn has a subtle inhibitory effect on the regeneration of action potentials. The action potential peaks decrease until after 60 s enough feedback is present to significantly reduce the action potentials, resulting in small amplitude V oscillations (< 20 mV amplitude and decreasing).

The oscillations in Fig. 3 A & B are more easily analysed if we plot how V and $[Ca^{2+}]_i$

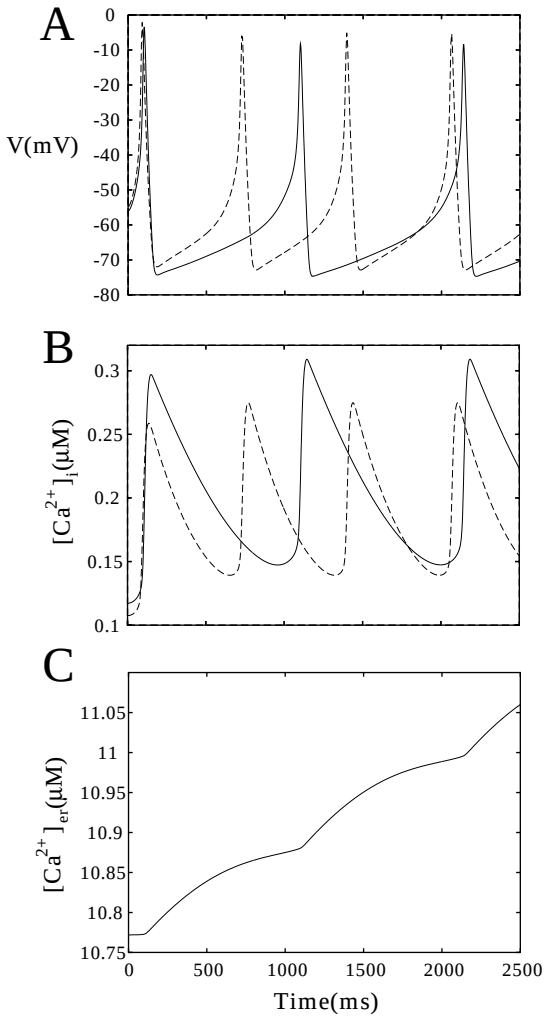

Figure 2: Comparison of the oscillatory phenomena in the ER model (—) with the original model (– – –). Indirect evidence supports a CRH-induced phosphorylation of the L-type Ca^{2+} channels, resulting in action potentials and Ca^{2+} transients. This phosphorylation is modeled by left-shifting the voltage dependence of the L-type Ca^{2+} current, V_{m_L}, from -12 mV to -18 mV, generating (A) action potentials, (B) $[Ca^{2+}]_i$ transients, and (C) a slow $[Ca^{2+}]_{er}$ increase.

change together over time (Fig. 4). The system starts from the point indicated by the $\star$, representing the model quiescent state. Time is represented by the line, progressing as both V and $[Ca^{2+}]_i$ change in value. From the quiescent state, both V and $[Ca^{2+}]_i$ start to increase. V soon peaks just below 0 mV, and then starts to repolarize as $[Ca^{2+}]_i$ increases further. Note that $[Ca^{2+}]_i$ increases greatly during the repolarization phase, because although the L-type Ca^{2+} current is being shut off as V falls, the driving force for Ca^{2+} is increasing. When V reaches its minimum value of -72 mV, the rise in $[Ca^{2+}]_i$ is complete, and V slowly ramps up as $[Ca^{2+}]_i$ falls. This represents the interspike interval. When V reaches about -60 mV, the next spike is initiated. Note that after the initial spike, the next several spikes follow a similar, but not identical, path. Viewed over a time period of up to about 10 s, the action

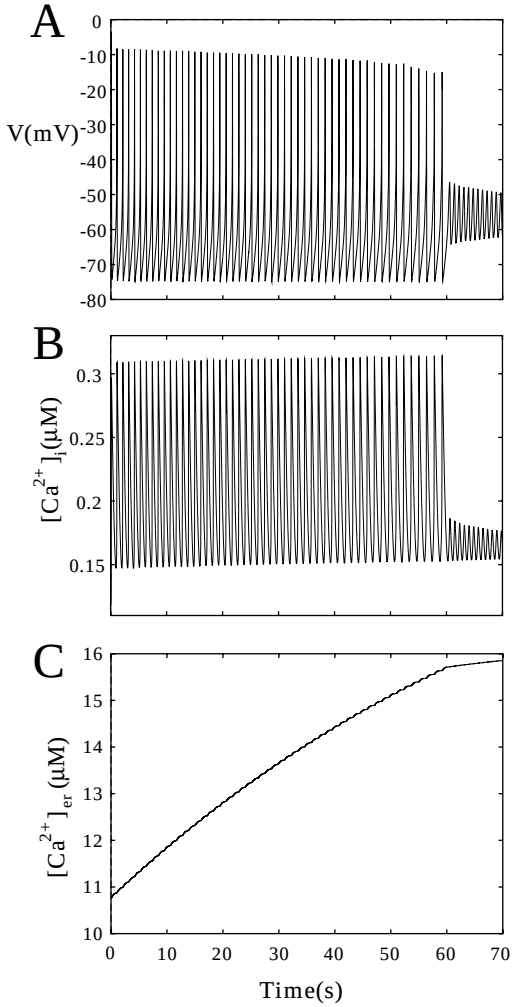

Figure 3: (A) ER model action potentials on a longer time scale to that of Fig. 2, generated by left-shifting the voltage dependence of the L-type Ca^{2+} current, V_{m_L}, from -12 mV to -18 mV. (B) There is a gradual rise in the $[Ca^{2+}]_i$, which increasingly activates the I_{K-Ca} current, inhibiting the action potentials. The action potential peaks decrease, until after 60 s enough feedback is present to significantly reduce the action potentials, resulting in small amplitude oscillations. (C) Coupled to the rise in $[Ca^{2+}]_i$ is a buildup of $[Ca^{2+}]_{er}$.

potentials appear to be stable, but Fig. 4 shows that each oscillation has a slightly larger average $[Ca^{2+}]_i$ value (i.e., average throughout one $[Ca^{2+}]_i$ transient cycle). This is because $[Ca^{2+}]_{er}$ is slowly rising (Fig. 3 C), and therefore J_{rel} is also slowly rising, releasing more Ca^{2+} during each oscillation. This in turn progressively increases the activation of the Ca^{2+}-activated K^+ channel, which affects the balance between the inward and outward currents that underlie the regeneration of action potentials. When $[Ca^{2+}]_{er}$, and thus the average $[Ca^{2+}]_i$ increase sufficiently, there is too much I_{K-Ca} current for another action potential to be generated. Instead small amplitude V oscillations occur (< 20 mV amplitude and decreasing). Ultimately stable oscillations are achieved, which have a V amplitude of 5 mV. Note that this effect (abolition of action potential activity) occurs due to a very minor increase

in $[Ca^{2+}]_i$, demonstrating the subtle interplay between the ER filling state and the plasma membrane electrical activity. Further, this effect shows that the ER can potentially play an important signaling role despite an initial appearance that it plays only a passive, buffering function during CRH-induced activity.

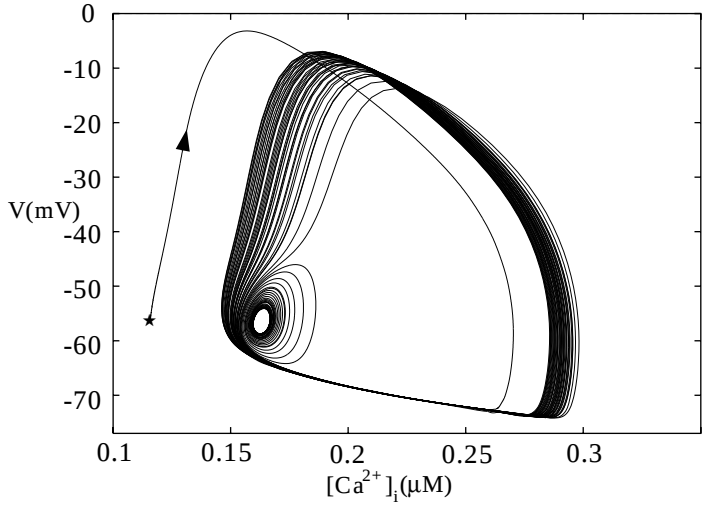

Figure 4: A left-shift in the voltage dependence of the L-type Ca^{2+} current V_{m_L} from -12 mV to -18 mV generates action potentials and associated $[Ca^{2+}]_i$ transients. The relationship between V and $[Ca^{2+}]_i$ during the oscillations is shown. The system starts from the previously quiescent state $\star$. The cycles move slowly to the right, indicating the gradual rise in $[Ca^{2+}]_i$. Ultimately stable oscillations are achieved, which have a V amplitude of 5 mV.

Experimental observations have shown that action potentials in response to application of CRH can persist for at least 15 min (Kuryshev et al., 1995b; Ritchie et al., 1996), indicating that the loss of action potentials we have observed in the ER model does not reflect a genuine physiological effect. However, it does seem physiologically reasonable that the ER should take up Ca^{2+} during repetitive $[Ca^{2+}]_i$ generation, which is the underlying cause of the model effect we have observed. This leads us to the question of how the cell avoids this model response when it would seem to have all the elements from which such an effect could arise. Obviously the model is a much simplified representation of the cells themselves, and the cells may have sophisticated mechanisms to prevent such an effect from occurring. However, within the confines of the model as it currently exists, we were interested in investigating ways in which action potential activity could be maintained despite a filling ER.

We tested the effects of changing various parameters on the ER model to see if the loss of action potential activity could be prevented. We determined that if the maximum plasma membrane Ca^{2+} pump rate, ν_p, is increased from 0.04 $\mu M \cdot \mu m \cdot ms^{-1}$ to 0.05 $\mu M \cdot \mu m \cdot ms^{-1}$ then, during repetitive action potential activity, $[Ca^{2+}]_{er}$ still rises but reaches a new, elevated, stable value of about $20\mu M$ without abolishing action potentials. The increased activity of the plasma membrane Ca^{2+} pump is able to prevent $[Ca^{2+}]_i$ from increasing to the level necessary to activate I_{K-Ca} and abolish action potential activity. The increase in the maximum pump rate is small and entirely reasonable, and in fact changes the resting (i.e., prior to the shift of V_{m_L}) membrane potential and $[Ca^{2+}]_i$ to -54.1 mV and 0.1 μM, respectively, values that are very similar to those from the original model.

Therefore a small and reasonable change in a single parameter can prevent the loss of action potentials, and in fact, appears to bring the ER model more into line with the original model (see below for further comparison). However, it seems unlikely that the cells would exist in a situation where a small perturbation in the level of expression of the plasma membrane Ca^{2+} pump (the cellular equivalent of reducing the maximum pump rate in the model) might lead to an inability to generate sustained firing of action potentials (as would happen in the model, if the maximum pump rate were reduced back to the original value of 0.4 $\mu M \cdot \mu m \cdot ms^{-1}$). The cell may therefore employ additional mechanisms to avoid, or at least reduce the possibility of, moving into a regime where repetitive firing would be compromised.

One well documented experimental observation in corticotrophs is a small depolarization, induced by CRH, which occurs prior to, and apparently independent of, firing of action potentials (Mollard et al., 1987; Kuryshev et al., 1995b; Kuryshev et al., 1996). These reports indicate that the depolarization is due to the reduction in a K^+ current. This current has recently been identified as an inward rectifier (Kuryshev et al., 1997), that is active at rest and its activity is reduced by CRH. Although no clear role for this effect has been determined, it could result in an increase in membrane excitability. We have previously simulated this effect and found that it did increase membrane excitability, but it did not seem to be obligatory for action potential generation (I).

We re-analysed the effects of simulating a reduction in a K^+ current that is active at rest by reducing the conductance of the leak current. We believe that that the inward rectifier current is a major component of the leak current. We found that with the maximum rate of the plasma membrane Ca^{2+} pump set to the original value of 0.04 $\mu M \cdot \mu m \cdot ms^{-1}$, reducing the leak conductance prevented the abolition of action potentials during sustained electrical activity. Therefore these results suggest that an integrated response to CRH (i.e., activation of the L-type Ca^{2+} current and inhibition of the inward rectifier, amongst other effects) may be employed to ensure that the cell is able to provide a sustained response for as long as it may be required.

Using the change in the maximum pump rate from 0.04 $\mu M \cdot \mu m \cdot ms^{-1}$ to 0.05 $\mu M \cdot \mu m \cdot ms^{-1}$, a 6 mV negative shift in the voltage-sensitivity parameter V_{m_L} generates sustained action potentials in the ER model, indicating that action potential generation occurs in the same way as it does for the original model. However to determine this with confidence and to investigate in more depth the behaviour of the system we subject the ER model to an analysis in which the behaviour is determined for V_{m_L} values that should encompass the physiologically relevant range. This is termed a bifurcation analysis, and is shown in Fig. 5 A, along with the bifurcation diagram for the original model (I) (Fig. 5 B). The resting, stable state of the model occurs at the right-hand side of the figures, at $V_{m_L} = -12$ mV, where the membrane potential is approximately -55 mV. As V_{m_L} is made progressively more negative the model retains stability (in electrophysiological terms the cell remains in its quiescent state) until $V_{m_L} = -17.72$ mV, a bifurcation point, whereupon action potentials emerge and the steady-state solution becomes unstable (- - -). The maximum and minimum values of the initially unstable periodic solution are indicated by the two branches extending from the bifurcation point ($\cdots$). These two branches arch backwards, and when the amplitude of the periodic solution reaches approximately 55 mV, the periodic solution becomes stable (—), i.e., repetitive action potentials are generated. The almost perpendicular arching of the unstable branches from the bifurcation point with respect to the steady state solution indicates that as observed experimentally, the repetitive model action potentials are generated in an all-or-none manner. As V_{m_L} is further decreased the amplitude of the periodic solution increases

more slowly. A slightly larger shift in $V_{\mathrm{m_L}}$ is required to generate action potentials in the ER model than in the original model, indicating that the ER model is slightly less excitable. This difference in model excitability is reflected in the bifurcation diagrams (Fig. 5), where the branching at the bifurcation point occurs at a more negative value of $V_{\mathrm{m_L}}$ for the ER model. Overall, we see that the behaviours of the original and ER models are very similar with respect to action potential generation.

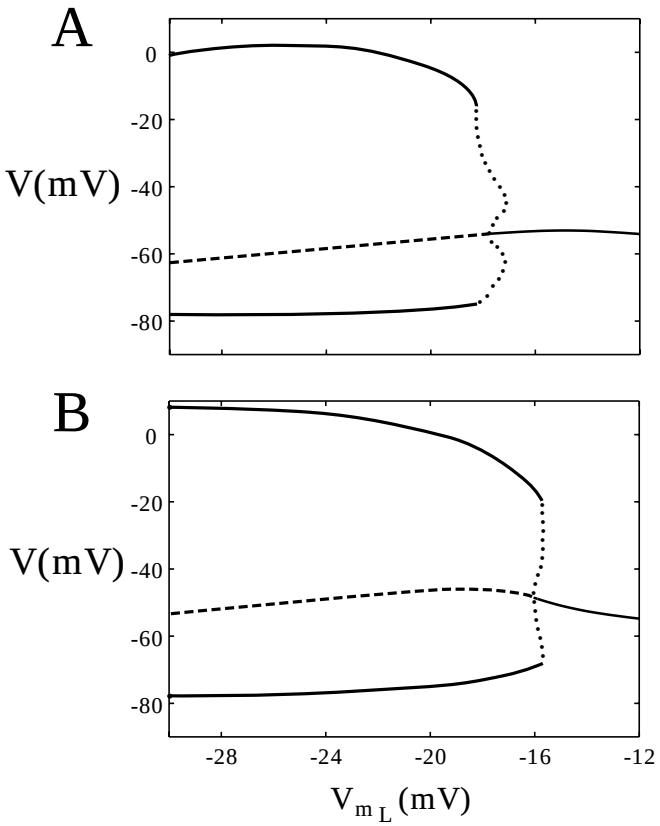

Figure 5: A comparison of the long term behaviour of the models for a range of $V_{\mathrm{m_L}}$ values: (A) The modified ER model, with a 25% larger plasma membrane pump rate $\nu_{\mathrm{p}} = 0.05\ \mu\mathrm{M} \cdot \mu\mathrm{m} \cdot \mathrm{ms}^{-1}$, and (B) the original model. This is termed a bifurcation analysis, and the upper and lower solid lines represent the max/min amplitude of the action potentials. A slightly larger shift in $V_{\mathrm{m_L}}$ is required to generate action potentials in the ER model than in the original model, indicating that the corticotroph cell model including the ER component is slightly less excitable.

The spatio-temporal calcium model

The spatio-temporal patterns in $[\mathrm{Ca}^{2+}]_{\mathrm{i}}$, generated by the subtle interplay between cellular Ca^{2+} sources and removal mechanisms, are a common mechanism of transmitting hormonal signals intracellularly (Meyer and Stryer, 1991). Because the Ca^{2+}-sensing components of the cell have both different sensitivities to Ca^{2+} and different spatial locations, we now consider the inclusion of spatial variation in the intracellular $[\mathrm{Ca}^{2+}]$. We introduce this structural

change in the model because it is believed to be an integral part of the exocytotic pathway, and may be important in the plasma membrane electrics (Meyer and Stryer, 1991). The spatial distribution of $[Ca^{2+}]_i$ is important in *Xenopus laevis* oocytes (Atri et al., 1993), and was considered in a model of gonadotrophs (Li et al., 1997). Consequently we now incorporate spatial variation in the cytosolic and endoplasmic $[Ca^{2+}]$ in the model. We model the cell as a spherical body, bounded by a plasma membrane, and assume that the ER is distributed homogeneously throughout the cell, sharing the intracellular volume with the cytosol. Furthermore, the distribution of pumps, channels and leaks is assumed to be uniform. The effects of cellular pump distribution on excitable cell electrical activity is not addressed here (see Sneyd and Sherratt, (1997) for a discussion of $[Ca^{2+}]_i$ wave propagation in inhomogeneous media).

The model

The partial differential equation governing $[Ca^{2+}]_i$ transport can be written as

$$\frac{\partial [Ca^{2+}]_i}{\partial t} = D_c \nabla^2 [Ca^{2+}]_i + \frac{f_{cyt}}{V_c}(J_{rel} - J_{up}), \tag{8}$$

where D_c is the effective diffusion coefficient for cytosolic Ca^{2+} and ∇^2 is the Laplacian operator, which under spherical symmetry has the form $r^{-2}\partial_r\big(r^2\partial_r\big)$. This equation is similar to Eq. 6. Again $\frac{f_{cyt}}{V_c}(J_{rel} - J_{up})$ represents the ionic transfer from the ER into the cytosol, and the term $D_c\nabla^2[Ca^{2+}]_i$ represents Ca^{2+} diffusion within the cytosol. It is important to observe that D_c is a function of the concentration of Ca^{2+} buffer sites, the buffering kinetics, and the $[Ca^{2+}]_i$. When the $[Ca^{2+}]_i$ is high, the Ca^{2+} buffers become saturated and the diffusion of Ca^{2+} is less impeded than for low $[Ca^{2+}]_i$. For $[Ca^{2+}]_i < 1.0$ μM, D_c can be assumed to have a constant value of 20 $\mu m^2 \cdot s^{-1}$ (Wagner and Keizer, 1994). The boundary condition for Eq. 8, is described by the flux condition

$$D_c \frac{\partial [Ca^{2+}]_i}{\partial r}\bigg|_{r=d_{cell}/2} = f_{cyt}(J_{in} - J_{eff}), \tag{9}$$

where $d_{cell} = 15$ μm, is the cell diameter. The construction of this boundary condition assumes that the Ca^{2+} flux near the plasma membrane is governed by Fick's law. The fraction of unbuffered cytosolic Ca^{2+}, f_{cyt}, near the plasma membrane is likely to be larger than 1%, and the Ca^{2+} diffusion coefficient near the plasma membrane is also likely to be nearer the unbuffered Ca^{2+} diffusion coefficient. However we do not incorporate this detail in our model. The ER dynamics are defined through an equation similar to (8), but the rate of concentration accumulation is now moderated by the factor f_{er}/V_{er}, so yielding

$$\frac{\partial [Ca^{2+}]_{er}}{\partial t} = D_{er}\nabla^2 [Ca^{2+}]_{er} - \frac{f_{er}}{V_{er}}(J_{rel} - J_{up}), \tag{10}$$

where D_{er} is the effective diffusion coefficient for ER Ca^{2+}. Because the concentration of Ca^{2+} buffer sites in the ER is several orders of magnitude larger than in the cytosol (Allbritton et al., 1992), it is expected that $D_{er} < D_c$. Interestingly, because the cell does not generate large $[Ca^{2+}]_{er}$ gradients and the ER predominantly acts as a Ca^{2+} storage facility rather than

a source of Ca^{2+}, the value of D_{er} (see Table 1) has very little effect on the model behaviour. It is assumed that the ER does not interact directly with the extracellular medium, i.e.,

$$D_{er}\frac{\partial[Ca^{2+}]_{er}}{\partial r}\bigg|_{r=d_{cell}/2} = 0. \tag{11}$$

The model assumes for simplicity that all Ca^{2+} buffers are immobile. It is important to note that the existence of even small amounts of mobile buffer alters the mass transport equations, introducing an extra non-diffusive term (Wagner and Keizer, 1994) into Eq. 8 and Eq. 10. However we do not present here a model including this extra complexity.

Numerical Methods

The system of partial differential equations (Eqs. 8-11), along with Eq. 1 and the equations associated with the channel activation gating variables (I), were solved by the method of lines (Schiesser, 1994) using a stiff system solver in the numerical package XPPAUT(3.0). Various discretisations of the partial differential equations, ranging from coarse (5 shells of equal thickness) to fine (100 shells) were implemented. The figures in this paper were generated using a model discretisation of 20 shells, allowing sufficient accuracy without excessive computation.

The model behaviour

As more realistic Ca^{2+} handling has been incorporated in the model, we wish to verify the mechanisms of action potential generation established previously. The inclusion of spatial variation in the intracellular $[Ca^{2+}]$ in the model does not affect the equilibrium state; at rest the $[Ca^{2+}]_i = 0.1$ μM, $[Ca^{2+}]_{er} = 8.48$ μM and the membrane potential $V = -54.1$ mV. As before, to simulate the proposed PKA-induced shift in the voltage sensitivity of the L-type current, we left-shift V_{m_L}, the voltage at which the L-type current is half-maximally activated. This left-shift in V_{m_L} from -12 mV to -18 mV generates action potentials, with associated $[Ca^{2+}]_i$ transients (Fig. 6). The action potentials (—) exhibit a similar form when compared with those from the ER model (– – –), with a decrease in both the period and the amplitude of oscillation. $[Ca^{2+}]_i$ transients near the plasma membrane (—), and at the cell centre (– — –), display faster and slower falling phases respectively when compared with $[Ca^{2+}]_i$ transients in the ER model (– – –). Both models exhibit a slow $[Ca^{2+}]_{er}$ increase. The similarity of the bifurcation diagrams (not shown) for the spatio-temporal Ca^{2+} model and the ER model indicates that the characteristics of action potential generation are similar.

The cytosolic Ca^{2+} diffusive flux is small relative to the average Ca^{2+} flux through the plasma membrane during an action potential. Hence there exists a high $[Ca^{2+}]_i$ gradient within the cell. $[Ca^{2+}]_i$ levels near the plasma membrane are typically higher than average $[Ca^{2+}]_i$ levels (Fig. 7). The combination of the high $[Ca^{2+}]_i$ gradient, and Ca^{2+} diffusion, generates diffusive $[Ca^{2+}]_i$ waves traveling from the cell boundary to the cell centre (Fig. 7). Due to Ca^{2+} buffering and Ca^{2+} uptake by the ER, these diffusive waves undergo severe damping as they travel toward the centre of the cell. This $[Ca^{2+}]_i$ gradient does not significantly affect the generation of action potentials, so we conclude that at present, the simple lumped cytosolic Ca^{2+} description seems sufficient to explain plasma membrane electrical activity. The ordinary differential equation model description is also more convenient to use and easier to understand.

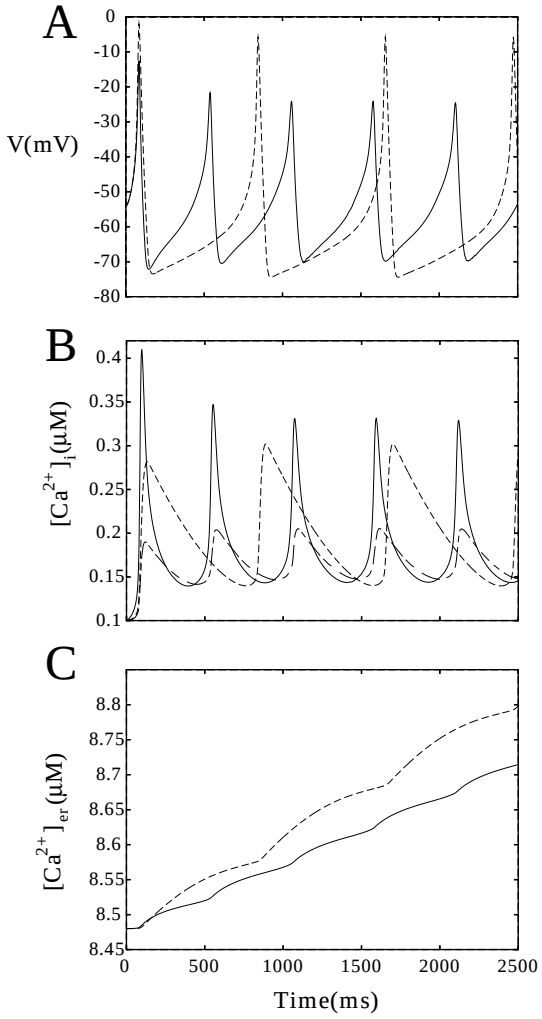

Figure 6: Comparison of the action potentials and $[Ca^{2+}]_i$ transients for the spatio-temporal Ca^{2+} model, and the modified ER model with $\nu_p = 0.05\ \mu M \cdot \mu m \cdot ms^{-1}$. (A) A left-shift in the voltage dependence of the L-type Ca^{2+} current, V_{m_L}, from -12 mV to -18 mV generates action potentials in the spatio-temporal Ca^{2+} model (—), which display similar kinetic features to those in the ER model (– – –). (B) $[Ca^{2+}]_i$ transients near the plasma membrane (—), and at the cell centre (– — –), display faster and slower falling phases respectively when compared with $[Ca^{2+}]_i$ transients in the ER model (– – –). (C) The ER model (– – –) exhibits a slower $[Ca^{2+}]_{er}$ increase than the spatio-temporal Ca^{2+} model (—).

Proposed experiment to test model predictions

Both the ER model and the spatio-temporal model predict a considerable rise in $[Ca^{2+}]_{er}$ during repetitive action potential activity and that this, in principle, could signal back to the plasma membrane and influence electrical activity. The extent of the rise in $[Ca^{2+}]_{er}$ would be an important determinant of the level of influence of such a signal, and is therefore an important factor to consider. We propose, and simulate, a simple experiment that could be used to measure this factor.

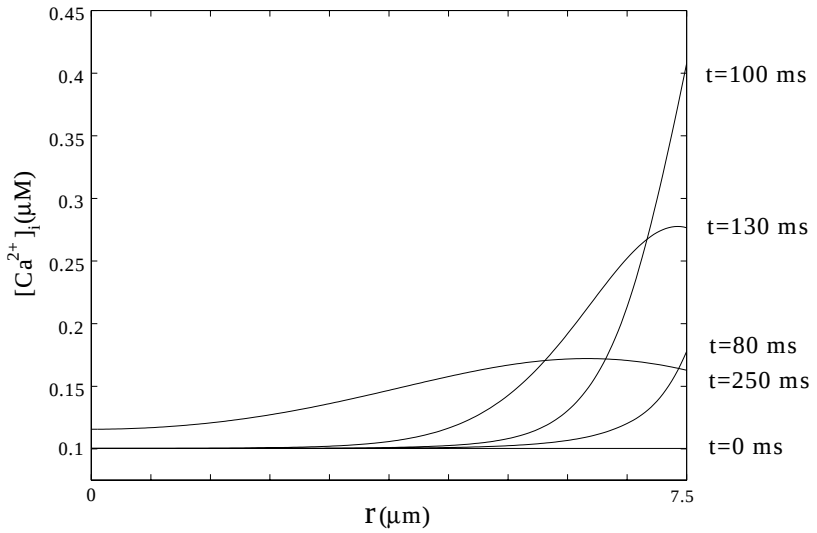

Figure 7: The spatial distribution of $[Ca^{2+}]_i$ during an action potential, at times 0, 80, 100, 130, and 250 ms. The horizontal coordinate r denotes the radial distance from the cell centre ($r = 0$) to the plasma membrane ($r = 7.5$ μm). The diffusive $[Ca^{2+}]_i$ wave traveling from the cell boundary to the cell centre is highly damped, due to Ca^{2+} buffering and ER Ca^{2+} uptake.

ER Ca^{2+} can be released into the cytosol by Ca^{2+} ionophores such as A23187 and ionomycin (Iono) (Corcuff et al., 1993; Won and Orth, 1995), and Ca^{2+} uptake into the ER can be inhibited by thapsigargin, an ER Ca^{2+}-ATPase inhibitor. To measure the amount of sequestered ER Ca^{2+} following CRH-induced activity, Iono could be applied, and the level of $[Ca^{2+}]_i$ compared with the same treatment without prior exposure to CRH. The results of this experiment simulated with our ER model are shown in Fig. 8, where a 40 s CRH application is elicited by a change in V_{m_L} from -12 mV to -18 mV, and the application of Iono is mimicked by a tenfold increase in the ER leak permeability P. As can be seen, there is a greater release of stored Ca^{2+} in the CRH-treated case. Some indication of the rate of Ca^{2+} accumulation in the ER could be obtained by varying the period of exposure to CRH. Although this is a simple experiment, the results of its execution would be valuable for testing the model predictions and for providing information on the role of the ER during action potential activity.

Discussion

To investigate mechanisms by which CRH induces membrane electrical activity, we describe in this paper an extension to our model of corticotroph electrical activity (I) by investigating more realistic intracellular Ca^{2+} mechanisms (addition of a distinct ER compartment allowing bidirectional exchange of Ca^{2+} with the cytosol) and the resulting effects on the model dynamics. Using this model we have found that an increase in the L-type Ca^{2+} current is sufficient to initiate repetitive action potentials from a previous quiescent model state. It must be emphasized that our hypothesis of action potential generation via a PKA-induced enhancement of the L-type Ca^{2+} current remains valid in the more physiological model. Ex-

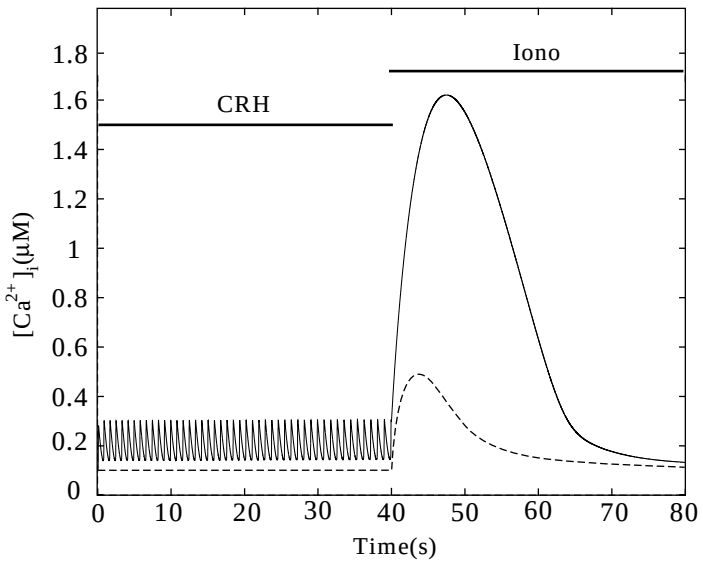

Figure 8: The magnitude of $[Ca^{2+}]_{er}$ increase during CRH application is undetermined. Application of an ionophore such as ionomycin (Iono) after an application of CRH would indicate the amount of Ca^{2+} sequestered by the ER during CRH application. A 40 s CRH application is elicited by a change in V_{m_L} from -12 mV to -18 mV, and is followed by an application of ionomycin(—), mimicked by a tenfold increase in the ER leak permeability P. The degree of ER Ca^{2+} uptake is apparent from a comparison with cells subjected to only ionomycin (– – –).

perimental investigation is necessary to determine whether the PKA enhancement of the L-type Ca^{2+} current occurs by an increase in the macroscopic current of the L-type channel, or by inducing a left-shift in the voltage sensitivity of the L-type channel. Reports from other cell types have indicated that PKA can induce a left-shift of $6-10$ mV in the voltage sensitivity of the L-type current. Shifts within this experimentally observable range induced repetitive model action potentials in an all-or-none manner as observed experimentally.

We found that during repetitive action potential activity, the ER sequesters Ca^{2+} and therefore acts as a buffer for $[Ca^{2+}]_i$. However, for our original parameter choices and Ca^{2+} exchange mechanisms action potential activity was eventually lost due to excessive feedback release of Ca^{2+} from the ER causing an increase in the activity of I_{K-Ca}, which in turn reduced membrane excitability sufficiently to prevent further action potential generation. We do not believe this to be a response normally found in corticotrophs, and the effect can be eliminated by small and reasonable parameter changes. However the underlying mechanisms seem valid and so there would appear to be some risk to the cells that they could not faithfully generate a sustained cellular response to CRH exposure. This suggests that corticotrophs employ strategies to prevent such an effect from occurring. We tested the potential role of CRH-induced reduction of an inward rectifier K^+ current, an effect observed experimentally by Kuryshev et al., 1997. We achieved this by reducing the conductance of the model leak current, and we found that this change prevented the loss of action potential activity. This reduction in the inward rectifier K^+ current may represent one of many strategies employed by corticotrophs to ensure a sustained cellular response to CRH.

The spatial distribution of Ca^{2+} is important in other cell types. Consequently we incor-

porated spatial variation in the cytosolic and endoplasmic Ca^{2+} in the model. The resulting model action potentials and Ca^{2+} transients exhibit a similar form when compared with previous models. Model $[Ca^{2+}]_i$ levels near the plasma membrane were typically higher than average $[Ca^{2+}]_i$ levels. This high $[Ca^{2+}]_i$ gradient, combined with Ca^{2+} diffusion, generates highly damped diffusive $[Ca^{2+}]_i$ waves traveling from the cell boundary to the cell centre. This $[Ca^{2+}]_i$ gradient did not have a significant impact on the generation of action potentials, so we conclude that at present, the simple lumped cytosolic Ca^{2+} description is sufficient to explain plasma membrane electrical activity. However the spatial variation in Ca^{2+} may be important in modeling aspects of the secretion process. The simple lumped cytosolic Ca^{2+} model description is also more convenient to use and easier to understand.

The present study represents a step in a project to construct a model describing the major aspects of the regulation of ACTH secretion in response to CRH and other ACTH regulators. Many of the intricate details surrounding Ca^{2+} signaling and the CRH-induced exocytotic pathway remain to be resolved. This paper aims to highlight aspects of the cellular regulation that can be tested experimentally in order to resolve some of these outstanding issues in corticotroph cell function.

This work was supported by grants from the New Zealand Lottery Grants Board (AP047957), the Marsden Fund administered by the Royal Society of New Zealand, and (PRS) acknowledges the receipt of a University of Canterbury doctoral scholarship. We also thank S.W. Slater for helpful discussions.

References

Aguilera, G., J. P. Harwood, J. X. Wilson, J. H. Morell, J. H. Brown, and K. J. Catt, 1983. Mechanisms of action of corticotropin release in rat pituitary cells. *J. Biol. Chem.* 258:8039–8045.

Alberts, B., D. Bray, J. Lewis, M. Kaff, K. Roberts, and J. D. Watson, 1983. Molecular Biology of the Cell. Garland, New York, 1st edition.

Allbritton, N. L., T. Meyer, and L. Stryer, 1992. Range of messenger action of calcium ion and inositol 1,4,5-triphosphate. *Science.* 258:1812–1815.

Antoni, F. A., 1986. Hypothalmic control of andrenocorticotropin secretion: Advances since the discovery of 41-residue corticotropin releasing factor. *Endocr. Rev.* 7:351–378.

Atri, A., J. Amundson, D. E. Clapham, and J. Sneyd, 1993. A single-pool model for intracellular calcium oscillations and waves in the *Xenopus laevis* oocyte. *Biophys. J.* 65:1727–1739.

Bilezikjian, L. M. and W. W. Vale, 1983. Glucocorticoids inhibit corticotropin releasing factor induced production of cAMP in cultured anterior pituitary cells. *Endocrinology.* 113:657–662.

Clapham, D. E., 1995. Calcium signaling. *Cell.* 80:259–268.

Corcuff, J. B., N. C. Guérineau, P. Mariot, B. T. Lussier, and P. Mollard, 1993. Multiple cytosolic calcium signals and membrane electrical events evoked in single arginine vasopressin-stimulated corticotrophs. *J. Biol. Chem.* 268:22313–22321.

Doedel, E., 1981. A program for the automatic bifurcation analysis of autonomous systems. *Congr. Numer.* 30:265–484.

Gibbs, D. M., 1985. Inhibition of corticotropin release during hypothermia: the role of corticotropin releasing factor, vasopressin, and oxytocin. *Endocrinology.* 116:723–727.

Guérineau, N. C., J. B. Corcuff, P. Mariot, B. T. Lussier, and P. Mollard, 1991. Spontaneous and corticotropin-releasing factor-induced cytosolic calcium transients in corticotrophs. *Endocrinology.* 129:409–420.

Hille, B., 1992. Ionic Channels of Excitable Membranes. Sinauer, Sunderland, MA., 2nd edition.

Hodgkin, A. L. and A. F. Huxley, 1952. A quantitative description of membrane current and its application to conduction and excitation in nerve. *J. Physiol. (Lond).* 117:500–544.

Jafri, M. S. and J. Keizer, 1995. On the roles of Ca^{2+} diffusion, Ca^{2+} buffers, and the endoplasmic reticulum in IP_3 induced Ca^{2+} waves. *Biophys. J.* 69:2139–2153.

Jones, M. T. and B. Gillham, 1988. Factors involved in the regulation of adrenocorticotropic hormone/β-lipotropic hormone. *Physiol. Rev.* 68:743–818.

Keller-Wood, M. E. and M. F. Dallman, 1984. Corticosteriod inhibition of ACTH release. *Endocr. Rev.* 5:1–24.

Kuryshev, Y., G. V. Childs, and A. K. Ritchie, 1995a. Three high threshold calcium channel subtypes in rat corticotrophs. *Endocrinology.* 136:3916–3924.

Kuryshev, Y. A., G. V. Childs, and A. K. Ritchie, 1995b. Corticotropin-releasing hormone stimulation of Ca^{2+} entry in corticotrophs is partially dependent on protein kinase A. *Endocrinology.* 136:3925–3935.

Kuryshev, Y. A., G. V. Childs, and A. K. Ritchie, 1996. Corticotropin-releasing hormone stimulates Ca^{2+} entry through L- and P-type Ca^{2+} channels in rat corticotrophs. *Endocrinology.* 137:2269–2277.

Kuryshev, Y. A., L. Haak, G. V. Childs, and A. K. Ritchie, 1997. Corticotropin releasing hormone inhibits an inwardly rectifying potassium current in rat corticotrophs. *J. Physiol. (Lond).* 502.2:265–279.

Labrie, F., R. Vielluex, G. LeFerve, D. H. Coy, J. Sueiras-Diaz, and A. V. Schally, 1982. Corticotropin-releasing factor stimulates accumulation of adenosine 3',5'-monophosphate in rat pituitary corticotrophs. *Science* 216:1007–1008.

LeBeau, A., A. Robson, A. McKinnon, R. Donald, and J. Sneyd, 1997. Generation of action potentials in a mathematical model of corticotrophs. *Biophys. J.* 73:1263–1275.

Li, Y., J. Rinzel, L. Vergara, and S. Stojilković, 1995. Spontaneous electrical and calcium oscillations in unstimulated pituitary gonadotrophs. *Biophys. J.* 69:785–795.

Li, Y., S. Stojilković, J. Keizer, and J. Rinzel, 1997. Sensing and refilling calcium stores in an excitable

cell. *Biophys. J.* 72:1080–1091.

Luini, A., D. Lewis, S. Guild, D. Corda, and J. Axelrod, 1985. Hormone secretagogues increase cytosolic calcium by increasing cAMP in corticotropin-secreting cells. *Proc. Natl. Acad. Sci. USA* 82:8034–8038.

Lytton, J., M. Westlin, S. E. Burk, G. E. Shull, and D. H. Maclennan, 1992. Functional comparisons between isoforms of the sacroplasmic or endoplasmic reticulum family of calcium pumps. *J. Biol. Chem.* 267:14483–14489.

Merchenthaler, I., M. A. Hynes, S. Vigh, A. V. Schally, and P. Petrusz, 1984. Corticotropin releasing factor (CRF): Origin and course of afferent pathways to the median eminence (ME) of the rat hypothalamus. *Neuroendocrinology* 39:296–306.

Meyer, T. and L. Stryer, 1991. Calcium spiking. *Annu. Rev. Biophys. Biophys. Chem.* 20:153–174.

Mollard, P., N. C. Guérineau, J. Audin, and B. Dufy, 1987. Electrical properties of cultured human adrenocorticotropin-secreting adenoma cells: effects of high K^+, corticotropin-releasing factor, and angiotensin II. *Endocrinology.* 121:395–409.

Mundiña-Weilenmann, C., J. Ma, E. Ríos, and M. M. Hosey, 1991. Dihydropyridine-sensitive skeletal muscle Ca channels in polarized planer bilayers. *Biophys. J.* 60:902–909.

Nargeot, J., J. M. Nerbonne, J. Engels, and H. A. Lester, 1983. Time course of the increase in the myocardial slow inward current after a photochemically generated concentration jump of intracellular cAMP. *Proc. Natl. Acad. Sci. USA* 80:2395–2399.

Neher, E. and G. J. Augustine, 1992. Calcium gradients and buffers in bovine chromaffin cells. *J. Physiol. (Lond).* 450:273–301.

Plotsky, P. M., T. O. Bruhn, and W. W. Vale, 1985. Evidence for multifactor regulation of the andrenocorticotropin secretory response to hemodynamic stimuli. *Endocrinology.* 116:633–639.

Plotsky, P. M. and P. E. Sawchenko, 1987. Hypophysial-portal plasma levels, median eminence content, and immunohistochemical staining of corticotropin-releasing factor, arginine vasopressin, and oxytocin after pharmacological adrenalectomy. *Endocrinology.* 120:1361–1369.

Reisine, T., G. Rougon, and J. Barbet, 1986. Liposome delivery of cyclic AMP-dependent protein kinase inhibitor into intact cells: Specific blockade of cyclic AMP-mediated adrenocorticotropin release from mouse anterior pituitary tumor cells. *J. Cell Biol.* 102:1630–1637.

Ritchie, A. K., Y. A. Kuryshev, and G. V. Childs, 1996. Corticotropin-releasing hormone and calcium signaling in corticotrophs. *TEM* 7:365–369.

Rivier, C. L. and P. M. Plotsky, 1986. Mediation by corticotropin releasing factor (CRF) of adenohypophysial hormone secretion. *Ann. Rev. Physiol.* 48:475–494.

Rivier, C. L. and W. W. Vale, 1983. Modulation of stress-induced ACTH release by corticotropin-releasing factor, catecholamines and vasopressin. *Nature* 305:325–327.

Schiesser, W., 1994. Computational Mathematics in Engineering and Applied Sciences: ODE's, DAE's, PDE's. CRC Press, Boca Raton, FL.

Sculptoreanu, A., T. Scheuer, and W. Catterall, 1993. Voltage-dependent potentiation of L-type Ca^{2+} channels due to phosphorylation by cAMP-dependent protein kinase. *Nature.* 364:240–243.

Sneyd, J. and J. Sherratt, 1997. On the propagation of calcium waves in an inhomogeneous medium. *SIAM J. Appl. Math.* 57:73–94.

Takano, K., J. Yasufukutakano, A. Teramoto, and T. Fujita, 1996. Corticotropin-releasing hormone excites adrenocorticotrophic-secreting human pituitary adenoma cells by activating a nonselective cation current. *J. Clin. Invest.* 98:2033–2041.

Tse, A., F. W. Tse, and B. Hille, 1994. Calcium homeostasis in identified rat gonadotrophs. *J. Physiol. (Lond).* 477.3:511–525.

Tsien, R. W. and R. Y. Tsien, 1990. Calcium channels, stores and oscillations. *Annu. Rev. Cell Biol.* 6:715–760.

Wagner, J. and J. Keizer, 1994. Effects of rapid buffers on Ca^{2+} diffusion and Ca^{2+} oscillations. *Biophys. J.* 67:447–456.

Whitnall, M. H., E. Mezey, and H. Gainer, 1985. Co-localization of corticotropin-releasing factor and vasopressin in median eminence neurosecretory cells. *Nature* 317:248–250.

Widmaier, E. P. and M. F. Dallman, 1984. The effects of corticotropin-releasing factor on adreno-

corticotropin secretion from perfused pituitaries *in vivo*: Rapid inhibition by glucocorticoids. *Endocrinology.* 115:2368–2374.

Won, J. G. S. and D. N. Orth, 1995. Role of inositol triphosphate-sensitive calcium stores in the regulation of adrenocorticotropin secretion by perfused rat anterior pituitary cells. *Endocrinology.* 136:5399–5408.